

Communication: An existence test for dividing surfaces without recrossing

Ryan Gotchy Mullen, Joan-Emma Shea, and Baron Peters

Citation: *The Journal of Chemical Physics* **140**, 041104 (2014); doi: 10.1063/1.4862504View online: <http://dx.doi.org/10.1063/1.4862504>View Table of Contents: <http://scitation.aip.org/content/aip/journal/jcp/140/4?ver=pdfcov>

Published by the AIP Publishing

Articles you may be interested in[Crossing the dividing surface of transition state theory. II. Recrossing times for the atom–diatom interaction](#)
J. Chem. Phys. **140**, 134304 (2014); 10.1063/1.4870039[Communication: Transition state theory for dissipative systems without a dividing surface](#)
J. Chem. Phys. **136**, 091102 (2012); 10.1063/1.3692182[Divide-and-conquer-based linear-scaling approach for traditional and renormalized coupled cluster methods with single, double, and noniterative triple excitations](#)
J. Chem. Phys. **131**, 114108 (2009); 10.1063/1.3211119[Microcanonical rates, gap times, and phase space dividing surfaces](#)
J. Chem. Phys. **130**, 164118 (2009); 10.1063/1.3119365[Does Ga H 5 exist?](#)
J. Chem. Phys. **123**, 204303 (2005); 10.1063/1.2121588



NEW Special Topic Sections

NOW ONLINE
Lithium Niobate Properties and Applications:
Reviews of Emerging Trends

AIP Applied Physics
Reviews

Communication: An existence test for dividing surfaces without recrossing

Ryan Gotchy Mullen,¹ Joan-Emma Shea,^{2,3} and Baron Peters^{1,2}

¹*Department of Chemical Engineering, University of California, Santa Barbara, California 93106, USA*

²*Department of Chemistry and Biochemistry, University of California, Santa Barbara, California 93106, USA*

³*Department of Physics, University of California, Santa Barbara, California 93106, USA*

(Received 22 November 2013; accepted 6 January 2014; published online 23 January 2014)

The claim that Grote-Hynes theory (GHT), when it provides accurate rates, is equivalent to multidimensional variational transition state theory (VTST) has been debated for decades with convincing arguments on both sides. For the two theories to be equivalent a perfect dividing surface with no recrossing must exist. We describe an easily implemented test employing deterministic microcanonical (NVE) trajectories which can identify situations where no perfect dividing surface exists and thereby potentially falsify the claim of equivalence. We use this test to reach data-supported conclusions about the relationship between GHT and VTST. © 2014 AIP Publishing LLC. [<http://dx.doi.org/10.1063/1.4862504>]

A central goal of reaction rate theory is to obtain simple dynamical models which accurately reflect the mechanism of complex barrier crossing processes. The simplest model is transition state theory (TST).¹ TST assumes (1) a dividing surface that separates reactants from products, (2) an equilibrium population of states on the dividing surface, and (3) a simple dynamics in which all trajectories crossing the dividing surface from reactant to product continue on to the product state without ever recrossing. If trajectories do recross the dividing surface, then the TST rate constant k_{TST} will overestimate the true rate constant k .² Time-dependent coordinate systems³ and reaction coordinates that explicitly include momentum space degrees of freedom^{4,5} can help eliminate recrossing, but TST is most easily implemented for static coordinate systems and dividing surfaces in configuration space. Therefore, our discussion is restricted to dividing surfaces of the type $q(\mathbf{x}) = q_{\ddagger}$, where $q(\mathbf{x})$ is a collective variable computed from atomic configurational coordinates \mathbf{x} and q_{\ddagger} is the value of the collective variable at the dividing surface. The variational transition state theory (VTST) seeks dividing surfaces with minimal recrossing to make TST rate estimates as accurate as possible.^{6–11}

When the dynamical bottleneck is a high saddle on the potential energy surface, a dividing surface with very few recrossings can be constructed based on a harmonic approximation to the potential energy surface.^{12,13} The nearly perfect dividing surface passes through the saddle point and is oriented perpendicular to the unstable vibrational mode in mass-weighted coordinates.¹⁴ The resulting multidimensional harmonic TST is widely used in chemical kinetics.

When the saddle has strong anharmonic features at the considered temperature or when transition paths can take numerous routes on a rugged energy landscape, a full configuration space optimization of $q(\mathbf{x}) = q_{\ddagger}$ is not feasible. In these cases the true coordinate independent rate constant k can be computed using an approximate dividing surface and reaction coordinate q as

$$k = \kappa[q] k_{\text{TST}}[q], \quad (1)$$

where the transmission coefficient $\kappa[q]$ is a correction for dynamical recrossing errors in $k_{\text{TST}}[q]$. κ can be obtained numerically from the reactive flux correlation functions using the full multidimensional dynamics.¹⁵ Alternatively, the one-dimensional models of Kramers theory¹⁶ and Grote-Hynes theory¹⁷ (GHT) invoke friction in the reaction coordinate dynamics to estimate the recrossing corrections. Kramers theory utilizes Markovian friction that implies the solvent instantly equilibrates to the reacting solute. GHT generalizes Kramers theory to account for more realistic solvent response times and non-Markovian friction. GHT has accurately estimated κ for solvated isomerizations,^{18,19} $\text{S}_{\text{N}}2$ reactions,^{20–22} dissociation reactions,^{23–28} and enzymatic catalysis.^{29,30}

GHT begins from a generalized Langevin equation (GLE) for the motion of a mass-weighted coordinate x

$$\ddot{x} = \omega^2 x - \int_0^t d\tau \eta(t - \tau) \dot{x}(\tau) + R, \quad (2)$$

where ω is the unstable frequency associated with a harmonic approximation to the potential of mean force $V(x)$ at the barrier top, R is a random force and η is a friction memory kernel which obeys the fluctuation-dissipation theorem

$$k_{\text{B}}T \eta(t) = \langle R(0)R(t) \rangle. \quad (3)$$

The brackets indicate a thermal average. In Eq. (2), the time-dependence of x and R has been omitted except where correlating quantities at two different times. The rate constant from GHT is the product of k_{TST} and a transmission coefficient κ_{GH}

$$\kappa_{\text{GH}} = \lambda/\omega, \quad (4)$$

where the reactive frequency λ is the largest, positive root to the GH equation

$$\lambda^2 + \lambda \tilde{\eta}(\lambda) - \omega^2 = 0. \quad (5)$$

$\tilde{\eta}(\lambda)$ is the frequency-dependent Laplace transform of the time-dependent friction $\eta(t)$. In practice computing κ_{GH} only requires $\eta(t)$ at $x = x_{\ddagger}$, which is evaluated from Eq. (3). It is important to note that GHT, in theory and in practice, does not

begin with an optimized reaction coordinate. The k_{TST} contribution changes with the choice of x , so if GHT is to give correct overall rates, $\eta(t)$ and κ_{GH} must also change with different choices of x .

An important connection between multidimensional TST and GHT is often illustrated with a harmonic saddle model where friction emerges from a bath of bilinearly coupled harmonic oscillator (BCHO) modes.^{12,18,19,31–37} The bath modes are combined with the potential of mean force $V(x)$ to form a multidimensional Hamiltonian

$$H = \frac{1}{2}p^2 + V(x) + \frac{1}{2} \sum_i \left[\dot{y}_i^2 + \omega_i^2 \left(y_i + \frac{c_i}{\omega_i^2} x \right)^2 \right], \quad (6)$$

which again starts from mass-weighted variables. p is the conjugate momentum to x , and y_i is the i th bath mode with frequency ω_i and coupling constant c_i . The Hamiltonian dynamics along x from Eq. (6) reduce to a GLE,³¹ with the friction given by the cosine series

$$\eta(t) = \sum_i \frac{c_i^2}{\omega_i^2} \cos(\omega_i t). \quad (7)$$

When $V(x)$ is again replaced with its harmonic approximation, $V(x) \approx V(x_{\ddagger}) - \omega^2 x^2/2$, then Eq. (6) becomes equivalent to Eq. (2), and moreover, Eq. (6) becomes exactly solvable by multidimensional TST.^{18,19,32,33} In the exact harmonic solution, the true reaction coordinate q —the unstable mode in the multidimensional space—mixes x with bath degrees of freedom. Recrossing is completely eliminated and the exact rate is obtained from TST without the transmission coefficient correction, as shown in Fig. 1(a).

In the case of the BCHO model, the GHT calculation effectively corrects for the choice of a non-optimal dividing surface. In fact, the demonstration that a BCHO model is exactly equivalent to GHT and exactly solvable by VTST has been interpreted by many to mean that a successful application of

GHT implies an underlying multidimensional BCHO model for which VTST would be exact. For example, Chandler has written that “GHT is a version of multidimensional transition state theory.”³⁸ Pollak commented “The equilibrium interaction of the bath with the system causes a change in the optimal transition state. Once this transition state is identified, there are no further corrections, dynamical or otherwise.”⁹ Truhlar and Garrett wrote “the success of GHT . . . means that VTST with a suitable choice of solvent coordinate and an optimization of the orientation of the dividing surface does remove the recrossing.”³⁹ This perspective is supported by studies of the $\text{S}_{\text{N}}2$ reaction $\text{Cl}^- + \text{CH}_3\text{Cl}$ in water, for which κ_{GH} was computed from a GLE, Eqs. (2) and (3),^{20–22} and identical κ_{GH} were later computed from a BCHO, Eqs. (6) and (7).⁴⁰ The “reaction coordinate” of GHT is defined using only solute degrees of freedom and any mechanistic role of the solvent is lumped into the dynamical transmission coefficient κ_{GH} . Therefore, the idea that VTST could specifically identify the mechanistic role of the solvent while also providing dynamically accurate rates is appealing.

However, Hynes argued that GHT is more general than VTST,³⁸ and that the BCHO model is perhaps not the only way to obtain the GLE.²² Dakhnovskii and Ovchinnikov espoused a similar perspective, noting “[BCHO] oscillators should be considered nonphysical. . . . We can only determine their combination which is equal to the memory function.”³² In atomistic systems, motion along the reaction coordinate under the PMF might be coupled to an anharmonic bath, a bath of inter-coupled oscillators, a bath possessing local intermediate traps (see Fig. 1(b)), or even to a system with multiple non-equivalent pathways all affecting the same transformation. Unfortunately, such highly nonlinear dynamics are not amenable to analytic projections, so there is no rigorous demonstration that the dynamics projected onto a coordinate would follow a second order GLE like that of Eq. (2). In several cases where GHT has been demonstrated to give accurate rates,^{23–30} it has not yet been possible to identify the solvent coordinates or optimize dividing surfaces, by VTST or by other means. It therefore remains difficult to determine whether recrossing emerges from a non-optimal reaction coordinate, or from some intrinsic friction related to nonlinearities in the dynamics.

The true origin of recrossing, in our view, depends on the system being investigated and on the coordinates being used. In developing simple models of complex barrier crossing processes, it would be useful to have a systematic test to determine whether friction-induced recrossing of the dividing surface can be eliminated by some better coordinate, or whether we should accept recrossing as inevitable and move forward with approximate GLE models of the dynamics.

VTST can provide exact rates with no further corrections only if a recrossing-free dividing surface exists. The claim that a no-recrossing surface exists has potentially falsifiable consequences. Suppose that a dividing surface exists in configuration space that is not recrossed by any deterministic trajectories. By definition, all trajectories initiated in A that reach the dividing surface must continue on to B. An A \rightarrow A trajectory cannot share a common configuration \mathbf{x} —coordinates of all atoms identical—with a B \rightarrow B trajectory. We refer to these

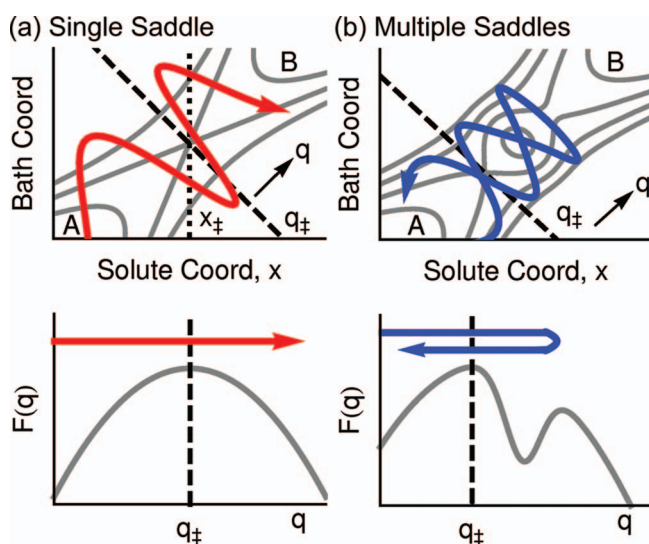


FIG. 1. Schematics of the upper panels depict deterministic trajectories on a two-dimensional model potential. In the lower panels, the trajectory and free energy F are projected onto the VTST coordinate q . (a) For a single, harmonic saddle, cf., Eq. (6), the $x = x_{\ddagger}$ surface has recrossing, but the $q = q_{\ddagger}$ surface does not. (b) An intermediate can cause trajectories to recross even the optimal dividing surface.

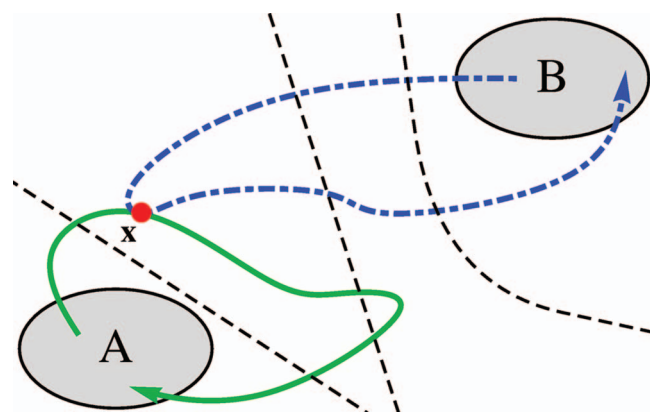


FIG. 2. Schematic of a system with two stable states A and B for which a recrossing pair, an $A \rightarrow x \rightarrow A$ trajectory (green) and a $B \rightarrow x \rightarrow B$ trajectory (blue, dotted-dashed), has been observed. Any possible dividing surface (e.g., black, dashed) is recrossed by the $A \rightarrow x \rightarrow A$ trajectory, the $B \rightarrow x \rightarrow B$ trajectory, or both.

$A \rightarrow x \rightarrow A$ and $B \rightarrow x \rightarrow B$ as recrossing pairs. The observation of a recrossing pair proves that a no-recrossing dividing surface cannot exist because all possible dividing surfaces are recrossed by the $A \rightarrow x \rightarrow A$ trajectory, the $B \rightarrow x \rightarrow B$ trajectory, or both, as shown in Fig. 2.

Note that, formally speaking, even one recrossing pair proves the non-existence of a perfect dividing surface at all temperatures.¹² A recrossing pair, once observed at some temperature, may be more or less important in the complete path ensemble⁴¹ at other temperatures, but it is a member of the complete path ensemble at all temperatures. In practice, trajectories with energies far above the activation energy have near-zero weight and negligible effects on the transmission coefficient.

Transition Path Sampling⁴² (TPS) provides one way to identify recrossing-pairs. In the TPS algorithm, a trial trajectory is generated from a randomly selected configuration, called a shooting point, on an existing transition path. If the trial trajectory is reactive, it is accepted and replaces the existing transition path. Each non-reactive trial trajectory is rejected in the sampling algorithm but could potentially be part of a recrossing-pair. Recrossing-pairs can be identified by tracking the outcomes (e.g., $A \rightarrow A$, $B \rightarrow B$) for all non-reactive trajectories initiated from each shooting point configuration. Microcanonical (NVE) versions of TPS should be used to identify recrossing pairs so that the dynamics are not altered by the stochastic thermostat.

Example 1: BCHO model. We first apply the test for recrossing-pairs to the BCHO model of Eq. (6). We anticipate that zero recrossing pairs will be observed because this model is proven to have a no-recrossing dividing surface.^{18,19,32,33} Using an inverted parabola $V(x) = -\omega^2 x^2/2$ and 11 bath modes with the parameters in Ref. 44, we have harvested 100 000 deterministic trajectories by a permutation shooting version of TPS with a 50% acceptance ratio (i.e., 50% were transition paths and the balance were non-reactive trajectories). All sampled trajectories have the same total energy $E = 11.5 k_B T$ relative to the saddle point potential, where the energy is measured in units such that $k_B T = 1.0$. Multiple trajectories were initiated from 19 651 configurations. Not a

single recrossing pair was observed from these data. For each configuration, there were either no non-reactive trajectories, all the non-reactive trajectories were $A \rightarrow A$, or all $B \rightarrow B$. In principle, the existence of a recrossing pair precludes a no-recrossing surface, but the absence of recrossing pair is not sufficient to prove existence of a perfect no-recrossing surface. In practice, when recrossing pairs are extremely rare, a fully variational dividing surface optimization should lead to accurate TST rates.

Example 2: Diffusive dynamics. We next consider a system with purely diffusive dynamics, or equivalently the limiting Kramers regime of large friction. In this limit, $\kappa \rightarrow 0$ and a no-recrossing surface is not possible. The expected number of recrossing pairs to be observed with Aimless Shooting can be calculated analytically using the committor p_B . p_B gives the probability that a trajectory initiated from x will relax to B.^{45,46} Since forward and backward trajectories from x are independent, the probability of generating a $B \rightarrow x \rightarrow B$ trajectory is p_B^2 and an $A \rightarrow x \rightarrow A$ is $(1 - p_B)^2$. The fraction of recrossing pairs at each value of p_B must be

$$f(p_B) = 2p_B^2(1 - p_B)^2. \quad (8)$$

f is sharply peaked near $p_B = \frac{1}{2}$. Shooting points from Aimless Shooting are distributed with statistical weight⁴³

$$p(p_B) \sim p_B(1 - p_B). \quad (9)$$

From Eqs. (8) and (9), the expected number of recrossing pairs is

$$\langle f \rangle = \frac{\int_0^1 dp_B f(p_B) p(p_B)}{\int_0^1 dp_B p(p_B)} = \frac{8.6 \text{ recrossing pairs}}{100 \text{ configurations sampled}}. \quad (10)$$

Example 3: Ion-pair dissociation. Finally, we consider an atomistic model of ion-pair dissociation in explicit solvent. Previous studies have confirmed the accuracy of GHT in predicting the rate of ion-pair dissociation.^{23,24} It has been proposed, specifically in the context of this system, that a dividing surface optimized by VTST might eliminate the recrossing.³⁹ As yet neither an accurate reaction coordinate nor a dividing surface without recrossing has been found. Therefore, ion-pair dissociation provides an ideal system to test for the existence of a no-recrossing surface.

We harvested 24 000 trial transition paths of an OPLS⁴⁷ NaCl ion-pair in TIP3P⁴⁸ water. Trajectories were computed in NAMD⁴⁹ using deterministic microcanonical (NVE) dynamics and periodic boundary conditions. The shooting point configuration and momenta for each trajectory were taken from a previous⁵⁰ Aimless Shooting simulation performed at constant temperature $T = 300$ K, pressure $P = 1$ bar, and number of water molecules $N = 394$. The volume V and energy E of each shooting point are different, but are held constant when propagating the system forward or backward in time for the present study. The timestep was 0.25 fs and the electrostatic energy was computed using Particle Mesh Ewald.⁵¹

Multiple trajectories were initiated from 4706 configurations and 419 recrossing pairs were observed. The ratio 8.9 recrossing pairs to 100 configurations sampled is similar in magnitude to Example 2, for which even a surface with

few recrossings is impossible. The approximate agreement is perhaps coincidental, because Ballard and Dellago showed that ion-pair dissociation trajectories have significant inertial character.⁵² Regardless, we can conclude that any trial dividing surface will have recrossings in a large portion of transition paths for this system. Clearly, the dynamical effects associated with ion-pair dissociation in explicit solvent cannot be eliminated by VTST. Because GHT provides an accurate transmission coefficient for ion-pair dissociation, this system provides a specific counterexample to the viewpoint that GHT and VTST have the same scope and underlying theoretical basis. Clearly GHT can (at least approximately) account for friction induced recrossings of nonlinear origins that cannot be removed by a dividing surface optimization.

In summary, many authors have asserted that an accurate rate constant from Grote-Hynes (GH) theory implies an underlying multidimensional system with a bilinearly coupled solvent for which VTST, if the appropriate solvent coordinates were known, would also become exact. This assertion has been difficult to support or refute with simulation data because of the extreme difficulties in optimizing dividing surfaces and reaction coordinates for reactions in solution. Here we note that VTST can only provide accurate rates—and therefore be equivalent to accurate GHT rates—when a surface with no recrossing exists. The assertion of an equivalence between GHT and VTST thus implies the existence of a no-recrossing surface, and the latter is potentially falsifiable. If a no-recrossing surface exists, then non-reactive trajectories containing an intermediate configuration \mathbf{x} must all terminate as either reactants (A) or as products (B). A pair of $A \rightarrow \mathbf{x} \rightarrow A$ and $B \rightarrow \mathbf{x} \rightarrow B$ trajectories sharing a common point \mathbf{x} is forbidden because any dividing surface would have to be crossed at least twice. We have studied two systems for which GHT is successful: a parabolic barrier bilinearly coupled to harmonic oscillators (BCHO) and atomistic ion-pair dissociation. Consistent with the well-known construction of a no-recrossing surface for the BCHO model, we observe no recrossing pairs. Transition path sampling data for ion-pair dissociation, however, reveals many recrossing pairs, proving that a no-recrossing surface (and even a surface with few recrossings) cannot exist. Because GHT does provide accurate transmission coefficients for ion-pair dissociation, our paper shows that GHT, contrary to some prior assertions, does have a broader scope of approximate validity than VTST.

This work was funded by the National Science Foundation (NSF): R.G.M. is supported by Graduate Research Fellowship No. DGE-1144085, B.P. is supported by CAREER Award No. 0955502, and J.E.S. is supported by Grant No. MCB-1158577. We used computing resources from the Center for Scientific Computing from the CNSI, MRL: an NSF MRSEC (DMR-1121053) and NSF CNS-0960316.

¹H. Eyring, *J. Chem. Phys.* **3**, 107–115 (1935).

²E. Wigner, *J. Chem. Phys.* **5**, 720–725 (1937).

³T. Komatsuzaki and R. Berry, *J. Mol. Struct. Theochem.* **506**, 55–70 (2000).

⁴T. Uzer, C. Jaffe, J. Palacian, P. Yanguas, and S. Wiggins, *Nonlinearity* **15**, 957 (2002).

⁵R. Hernandez, T. Uzer, and T. Bartsch, *Chem. Phys.* **370**, 270–276 (2010).

⁶J. C. Keck, *J. Chem. Phys.* **32**, 1035–1050 (1960).

⁷D. G. Truhlar and B. C. Garrett, *Acc. Chem. Res.* **13**, 440–448 (1980).

⁸D. G. Truhlar, W. L. Hase, and J. T. Hynes, *J. Phys. Chem.* **87**, 2664–2682 (1983).

⁹E. Pollak, *J. Chem. Phys.* **95**, 533–539 (1991).

¹⁰E. Vanden-Eijnden and F. A. Tal, *J. Chem. Phys.* **123**, 184103 (2005).

¹¹T. S. van Erp, *Adv. Chem. Phys.* **151**, 27–60 (2012).

¹²P. Hanggi, P. Talkner, and M. Borkovec, *Rev. Mod. Phys.* **62**, 251 (1990).

¹³K. J. Laidler, *Chemical Kinetics* (Harper and Row, Cambridge, 1987).

¹⁴D. G. Truhlar and B. C. Garrett, *J. Phys. Chem. A* **107**, 4006 (2003).

¹⁵D. Chandler, *J. Chem. Phys.* **68**, 2959 (1978).

¹⁶H. A. Kramers, *Physica* **7**, 284–304 (1940).

¹⁷R. F. Grote and J. T. Hynes, *J. Chem. Phys.* **73**, 2715–2732 (1980).

¹⁸G. van der Zwan and J. T. Hynes, *J. Chem. Phys.* **78**, 4174–4185 (1983).

¹⁹G. van der Zwan and J. T. Hynes, *Chem. Phys.* **90**, 21–35 (1984).

²⁰J. P. Bergsma, B. J. Gertner, K. R. Wilson, and J. T. Hynes, *J. Chem. Phys.* **86**, 1356–1376 (1987).

²¹B. J. Gertner, J. P. Bergsma, K. R. Wilson, S. Y. Lee, and J. T. Hynes, *J. Chem. Phys.* **86**, 1377–1386 (1987).

²²B. J. Gertner, K. R. Wilson, and J. T. Hynes, *J. Chem. Phys.* **90**, 3537–3558 (1989).

²³G. Ciccotti, M. Ferrario, J. T. Hynes, and R. Kapral, *J. Chem. Phys.* **93**, 7137–7147 (1990).

²⁴R. Rey and E. Guardia, *J. Phys. Chem.* **96**, 4712–4718 (1992).

²⁵L. X. Dang and D. E. Smith, *J. Chem. Phys.* **99**, 6950–6956 (1993).

²⁶L. X. Dang, G. K. Schenter, T.-M. Chang, S. M. Kathmann, and T. Autrey, *J. Phys. Chem. Lett.* **3**, 3312–3319 (2012).

²⁷P. T. M. Nguyen, V. T. Nguyen, H. V. R. Annappureddy, L. X. Dang, and D. Do, *Chem. Phys. Lett.* **554**, 90–95 (2012).

²⁸H. V. R. Annappureddy and L. X. Dang, *J. Phys. Chem. B* **117**, 8555–8560 (2013).

²⁹M. Roca, V. Moliner, I. Tunon, and J. T. Hynes, *J. Am. Chem. Soc.* **128**, 6186–6193 (2006).

³⁰J. J. Ruiz-Pernia, I. Tunon, V. Moliner, J. T. Hynes, and M. Roca, *J. Am. Chem. Soc.* **130**, 7477–7488 (2008).

³¹R. Zwanzig, *J. Stat. Phys.* **9**, 215–220 (1973).

³²Y. I. Dakhnovskii and A. A. Ovchinnikov, *Phys. Lett. A* **113**, 147–150 (1985).

³³E. Pollak, *J. Chem. Phys.* **85**, 865–867 (1986).

³⁴G. R. Haynes and G. A. Voth, *J. Chem. Phys.* **103**, 10176–10182 (1995).

³⁵G. A. Voth and R. M. Hochstrasser, *J. Phys. Chem.* **100**, 13034–13049 (1996).

³⁶G. K. Schenter, B. C. Garrett, and D. G. Truhlar, *J. Phys. Chem. B* **105**, 9672–9685 (2001).

³⁷J.-D. Bao, Y.-Z. Zhuo, F. A. Oliveira, and P. Hanggi, *Phys. Rev. E* **74**, 061111 (2006).

³⁸P. Barbara, J. T. Hynes, D. Chandler, M. C. R. Symons, M. H. Abraham, C. F. Wells, M. Henchman, M. J. Blandamer, D. Bush, K. H. Halawani, J. Schroeder, J. Troe, P. G. Wolynes, P. Suppan, H. L. Friedman, and D. G. Hall, *Faraday Discuss. Chem. Soc.* **85**, 341–364 (1988).

³⁹D. G. Truhlar and B. C. Garrett, *J. Phys. Chem. B* **104**, 1069–1072 (2000).

⁴⁰G. Gershinsky and E. Pollak, *J. Chem. Phys.* **103**, 8501–8512 (1995).

⁴¹J. Rogal and P. G. Bolhuis, *J. Chem. Phys.* **133**, 034101 (2010).

⁴²P. G. Bolhuis, D. Chandler, C. Dellago, and P. L. Geissler, *Annu. Rev. Phys. Chem.* **53**, 291–318 (2002).

⁴³B. Peters, G. T. Beckham, and B. L. Trout, *J. Chem. Phys.* **127**, 034109 (2007).

⁴⁴B. Peters, *Chem. Phys. Lett.* **554**, 248–253 (2012).

⁴⁵R. Du, V. S. Pande, A. Y. Grosberg, T. Tanaka, and E. S. Shakhnovich, *J. Chem. Phys.* **108**, 334–350 (1998).

⁴⁶P. L. Geissler, C. Dellago, and D. Chandler, *J. Phys. Chem. B* **103**, 3706–3710 (1999).

⁴⁷C. J. Fennell, A. Bizjak, V. Vlachy, and K. A. Dill, *J. Phys. Chem. B* **113**, 6782–6791 (2009).

⁴⁸W. L. Jorgensen, J. Chandrasekhar, J. D. Madura, R. W. Impey, and M. L. Klein, *J. Chem. Phys.* **79**, 926–935 (1983).

⁴⁹J. C. Phillips, R. Braun, W. Wang, J. Gumbart, E. Tajkhorshid, E. Villa, C. Chipot, R. D. Skeel, L. Kale, and K. Schulten, *J. Comput. Chem.* **26**, 1781–1802 (2005).

⁵⁰R. G. Mullen, J. E. Shea, and B. Peters, “Transmission coefficients, committers, and solvent coordinates in ion-pair dissociation,” *J. Chem. Theory Comput.* (to be published).

⁵¹T. Darden, D. York, and L. Pedersen, *J. Chem. Phys.* **98**, 10089–10092 (1993).

⁵²A. J. Ballard and C. Dellago, *J. Phys. Chem. B* **116**, 13490–13497 (2012).